Overlapping Azimuth Channels for SAR Imaging — Revisited

Marwan Younis, Nida Sakar, Marc Rodriguez-Cassola, Pau Prats-Iraola, Mariantonietta Zonno, Gerhard Krieger, and Alberto Moreira
Microwaves and Radar Institute, German Aerospace Center (DLR), Oberpfaffenhofen, Germany

Abstract

Digital beamforming in combination with multiple azimuth channels (MACs) enable high azimuth resolution and wide swath Synthetic Aperture Radar (SAR). In terms of the SAR trade space this comes at the expense of restricting the instrument Pulse Repetition Frequency (PRF) operation to values close to the uniform PRF values, determined by the ratio of total antenna length to platform velocity, or otherwise sacrificing, i.e., worsening the performance.
An approach, which has been investigated earlier, to change (increase) the uniform PRF while keeping the antenna length constant is to use overlapping azimuth channels. Here the analog RF output of individual azimuth antenna elements are assigned to two (or even more) digital channels. In this paper the impact of utilizing overlapping azimuth channels on the SAR instrument and performance parameters is analyzed. The aim is to establish a thorough understanding of the SAR trade space. A rigorous methodology is followed in developing closed form expressions to describe the relevant performance parameters.

1 Introduction

Synthetic Aperture Radar instruments equipped with Multiple Azimuth Channels (MACs) are known to attain a wide swath and fine azimuth resolution, the latter, as a consequence of covering a wide Doppler bandwidth combined with an adequate (azimuth) sampling of the radar echo data [1, 2]. The operation is such that the Doppler bandwidth of the radar echo signals is proportional to the antenna pattern's azimuth beamwidth on transmit, while the azimuth sampling on receive for any transmitted pulse is proportional to the number of digital channels. A proper planar, i.e, direct radiating, antenna design requires the transmit pattern's beamwidth to be approximately equal to that of each receive sub-array constituting a digital receive channel [3].

The radar sensor moves and successively transmits pulses at regular intervals known as the Pulse Repetition Interval (PRI). The azimuth samples' positions are a combination of the channel antenna sub-arrays' separation and the product of the PRI by the platform velocity. There is one specific Pulse Repetition Frequency (PRF) which results in equal spatial spacing between the azimuth samples known as the *uniform* PRF, which, for a contiguous planar array, is proportional to the total antenna length [1, 4]. It is desirable to operate the SAR instrument at, or at least close to, the uniform PRF; since any deviation results in noise scaling, i.e., a decreased Signal-to-Noise Ratio (SNR) and a degraded performance, predominantly the Azimuth Ambiguity to Signal Ratio (AASR). These effects manifest themselves in the processed SAR image and are obviously undesirable. The SAR data processing may equalize the worsened SNR or AASR but not both. On the other hand, practically it is not always possible to operate the instrument at the uniform PRF, because the timing is also determined by the intended position and width of the imaged swath, ground and orbit altitude (variations), and other parameters such as the required range ambiguity level. Moreover, burst imaging modes (such as ScanSAR or TOPS) inherently require different PRF values for each burst in order to image a contiguous swath.
The idea of introducing a sliding transmit window creating an overlap between the azimuth channels is not new and has been investigated thoroughly in [1] in the context of adapting the value of the uniform PRF during SAR operation. In this paper the topic is addressed on a conceptional level by considering a SAR instrument design with a fixed, i.e., non-adaptive, overlap between the azimuth channels. The aim is to gain a profound understanding of the trade-space (cf. also [5]) by investigating the effects (improvement or degradation) on the SAR instrument performance.

2 System Configuration and Model

The planar receive antenna array of the SAR instrument consists of N_{elm} contiguous antenna elements each of length L_{Rx} such that the total Rx antenna length is $L_{Rx} \cdot N_{elm}$.

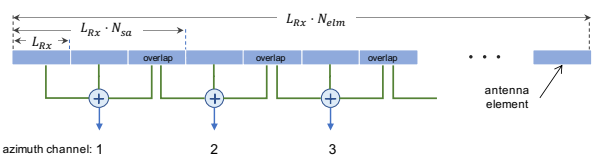

Figure 1: Antenna array configuration for the example case of $N_{sa} = 3$ and $N_{ov} = 1$.

The Rx antenna elements are connected to Transmit/Receive Modules (TRM) and a subsequent network which combines each group of N_{sa} elements into one digital azimuth channel. An overlap of N_{ov} elements is introduced between neighboring channels such that any two adjacent N_{sa}-element-groups have $0 \leq N_{ov} \leq N_{sa}$ elements in common, as shown in Fig. 1.

It is assumed that the individual signal and noise power levels are maintained, i.e., no additional additive (absorption) noise is introduced when implementing the overlap network. This results in equal signal and noise power levels across the input of the channel combiners. Although conservative, this assumption is justified by the high gain of the TRMs (each antenna element is connected to a TRM) and a proper amplification settings such that any subsequent noise contributions may be neglected.

For the analysis to follow and in order to ensure a fair comparison some parameter sets of the trade-space will be varied to observe the output performance while keeping some parameters fixed. Here the processed Doppler bandwidth and the pulse duty cycle are kept constant. The former implies that the azimuth resolution and the length of the sub-array constituting a channel, $L_{Rx} \cdot N_{sa}$, are fixed; while the later ensures a constant average transmit power (for a given TRM peak output power) which eliminates the number of TRMs from the trade-space. Further, the SAR transmit antenna beam pattern as well as any digital beamforming techniques applied in elevation, for example SCORE, are irrelevant and need not be taken into account.

The antenna system and subsequent network is described by the following equation [6] for the total number of elements:

$$N_{elm} = N_{ch}N_{sa} - N_{ov}(N_{ch} - 1) \tag{1}$$

with $N_{ch} \in \mathbb{N}$ the number of digital channels, $N_{sa} \in \mathbb{N}$ the number antenna elements per sub-array, and $N_{ov} \in \mathbb{N}$ the number of overlapping elements. The above equation may be recast to solve for the any of the four variables given the other three, and keeping in mind that the solution must always be an integer number.

Without restriction of generality it can be assumed that the transmit phase center is centered at the antenna. The combined phase center of the transmit and i-th receive antenna for the m-th transmit pulse then becomes:

$$p_c(i) = \frac{mv_{sat}T_{pri}}{2} + \left(i - \frac{N_{ch}-1}{2}\right)\frac{(N_{sa}-N_{ov})L_{Rx}}{2}, \tag{2}$$

for $i = 0 \ldots N_{ch} - 1$, where v_{sat} is the platform velocity, and $T_{pri} = 1/f_{prf}$ the pulse repetition interval (PRI). For any transmitted pulse the separation between any two adjacent phase centers, Δp_c, is constant at:

$$\Delta p_c = \frac{(N_{sa}-N_{ov})L_{Rx}}{2}, \tag{3}$$

Note that introducing an overlap $N_{ov} > 0$ will reduce the phase center separation, i.e., increase the spatial sampling.

2.1 Mathematical Signal Model

In the following we derive the expressions for the signal and noise power taking into account the overlap between the channels. Knowing that adding digital azimuth receive channels to a SAR instrument is equivalent to inserting (independent) azimuth samples, but does not increase the SNR of the raw data [3].

The SAR echo excites a signal s_i at antenna element $i = 1, 2, \ldots, N_{elm}$ received with an additive noise component n_i. In the following expressions for the signal and noise power of one digital channel, constituted of N_{sa} elements, are formulated.

2.1.1 Signal Power

The individual signal components are fully correlated when combined, since the sub-array pattern can be considered as a spatial filter limiting the signal's Doppler bandwidth. Thus $s_i = s \;\forall\, i$ and the element signal power is $E\{ss^*\} = \sigma_s^2$. The signal power of any one digital channel thus is:

$$\begin{aligned} P_s =& E\left\{\left(\sum_{i=1}^{N_{sa}} s_i\right)\left(\sum_{j=1}^{N_{sa}} s_j\right)^*\right\} \\ =& E\left\{N_{sa}sN_{sa}s^*\right\} = N_{sa}^2\sigma_s^2 \end{aligned} \tag{4}$$

2.1.2 Noise Power

The noise contribution to the elements, n_i, is modeled as independent and identically distributed random variables. The noise power (variance) of each element is $E\{n_i^2\} = \sigma_n^2 \;\forall\, i$. Due to the overlap the noise of the channels becomes partially correlated; to take this effect into consideration the single channel's noise power is computed as the channel-average of the total noise power, i.e., the total noise power divided by the number of channels. The resulting expression is:

$$\begin{aligned} P_n =& \frac{1}{N_{ch}} E\left\{\left(\sum_{i=0}^{N_{ch}-1}\sum_{j=1}^{N_{sa}} n_{(N_{sa}-N_{ov})\cdot i+j}\right)\right. \\ & \left.\left(\sum_{m=0}^{N_{ch}-1}\sum_{n=1}^{N_{sa}} n_{(N_{sa}-N_{ov})\cdot m+n}\right)^*\right\} \end{aligned} \tag{5}$$

Matrix Representations

It is convenient to simplify the above expression using matrix notation. Take an order N_{elm} row vector of which the first N_{sa} elements are 1 and the remaining $N_{elm} - N_{sa}$ elements are zero, thus $\mathbf{u} = [\mathbf{1}_{N_{sa}}^T, \mathbf{0}_{N_{elm}-N_{sa}}^T]$, where $\mathbf{1}_m$ and $\mathbf{0}_m$ are the null and one column vectors of order m, respectively. Define the *manifold vector* of channel $c = 1, \ldots, N_{ch}$ as the $(N_{sa} - N_{ov})(c-1)$ cyclic right shift of $\mathbf{u}$ such that $\mathbf{u}_c = [\mathbf{0}_{(N_{sa}-N_{ov})(c-1)}^T, \mathbf{1}_{N_{sa}}^T, \mathbf{0}_{N_{elm}-N_{sa}\cdot c}^T]$. The *array*

manifold matrix is defined as $\mathbf{U} = [\mathbf{u}_1, \mathbf{u}_2, \ldots, \mathbf{u}_{N_{ch}}]^T$. Then (5) may be written as:

$$P_n = \left(\|\mathbf{1}_{N_{ch}}^T \mathbf{U}\|_2\right)^2 \frac{\sigma_n^2}{N_{ch}} \tag{6}$$

where $\|\mathbf{x}\|_2$ is the L_2 or Euclidian norm of the vector $\mathbf{x}$. Note that in the case of no overlap $N_{ov} = 0$ and the noise power reduces to $\mathbf{1}_{N_{ch}}^T \mathbf{U} = \mathbf{1}_{N_{elm}}$ and $P_n = N_{elm}\sigma_n^2/N_{ch}$.

2.2 Azimuth Signal Reconstruction

A SAR instrument utilizing MACs and transmitting successive pulses at regular intervals, $T_{pri} = 1/f_{prf}$, will, in general, result in a periodic nonuniform sampling. Only for specific (uniform) PRF value, given by [6, 4]:

$$f_{prf}^{uni} = \frac{2v_{sat}}{N_{ch}(N_{sa} - N_{ov})L_{Rx}}, \tag{7}$$

the azimuth sampling will be regular. When $f_{prf} \neq f_{prf}^{uni}$ the azimuth signals need to be pre-processed to *reconstruct* the azimuth spectrum [6, 1, 2, 7] .

It is favorable to operate the SAR instrument close to the uniform PRF value. From (7) it is evident that utilizing overlapping channels provides for an additional degree of freedom, given by the parameter N_{ov}, to adjust the uniform PRF value.

It should, however, be noted that SAR systems operating in the burst mode, such as ScanSAR, two-burst ScanSAR, or TOPS [8, 9], will periodically change the PRF during a data take in order to allow for imaging a contiguous swath. Burst mode imaging will thus inherently operate at nonuniform PRF values at least for some bursts (the strategy developed in [10] allows adapting the uniform PRF during burst mode operation).

2.2.1 Signal-to-Noise Ratio Scaling

The azimuth spectrum of a periodic nonuniformly sampled signal can be reconstructed, however it is more sensitive to additive white noise than uniform sampling. The signal-to-noise (SNR) scaling factor quantifies the loss in SNR after the reconstruction due to the noise amplification [11, 1].

A closed expression for the SNR scaling due to periodic nonuniform temporal sampling is derived in [12, 13]. The expression can be applied to a MACs instrument after converting the spatial azimuth sampling to the equivalent temporal sampling, i.e., it to a equivalent single Tx/Rx antenna instrument with the identical periodic nonuniform sample's positions. With (2) and $\tau_i = p_c(i)/v_{sat}$ the expression in [12] for the SNR scaling factor, A_ϵ, becomes:

$$A_\epsilon = \frac{1}{N_{ch}} \sum_{l=0}^{N_{ch}-1} \frac{\sum_{k=0}^{N_{ch}-1} \prod_{\substack{i=0 \\ i\neq l}}^{N_{ch}-1} \cos^2 \pi \left(\frac{k - \gamma\left(i - \frac{N_{ch}-1}{2}\right)}{N_{ch}} \right)}{\prod_{\substack{i=0 \\ i\neq l}}^{N_{ch}-1} \sin^2 \pi \frac{(i-l)\gamma}{N_{ch}}} \tag{8}$$

where $\gamma = f_{prf}/f_{prf}^{uni}$ is a measure of the instrument PRF nonuniformity.

Fig. 2 shows the SNR scaling versus the sampling nonuniformity (here equivalent to the oversampling) according to (8). It is seen that for oversampling values in the order of 5 % to 10 % the SNR scaling remains reasonably low. For $\gamma = N_{ch}/(N_{ch} - 1) = 125\,\%$ a singularity occurs [10], because samples of successive transmit pulses overlap[1], causing a rapid increase in the A_ϵ.

Nevertheless, the increase in SNR shown in Fig. 2 is a worst case, since (8) assumes the processed Doppler bandwidth to be equal to the maximum possible value given by $N_{ch}f_{prf}^{uni}$ [12] and thus neglects any SNR improvement when processing to coarser azimuth resolution (an extensive analysis of the SNR scaling is given in [10]).

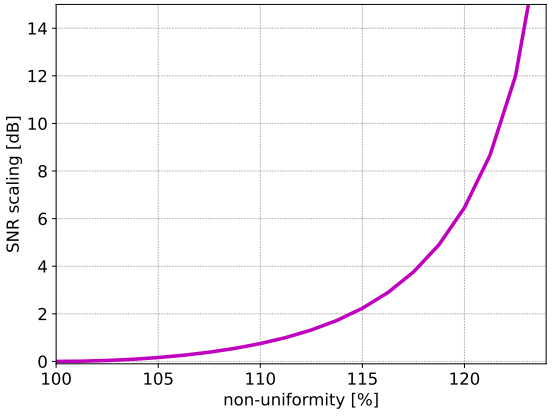

Figure 2: SNR scaling of a MACs system versus percentage nonuniformity γ. Here $\gamma = 100\,\%$ corresponds to the uniform PRF $f_{prf} = f_{prf}^{uni}$. The example MACs instrument has $N_{ch} = 5$ channels and $N_{sa} = 30$ sub-array antenna elements.

.

3 Performance Evaluation

In the following analysis the overlap is varied between $0 \leq N_{ov} \leq N_{sa}$, affecting the total antenna length $L_{Rx}N_{elm}$, while both the channel aperture length $L_{Rx} \cdot N_{sa}$ and the number of channels N_{ch} are fixed.

3.1 SNR Degradation due to Overlap

The channel SNR versus the percentage aperture overlap between the channels is shown in Fig. 3. Here the

[1]The singularity can be avoided by neglecting overlapping azimuth samples, however, this is not an "economical" instrument design.

abscissa is $N_{ov} \cdot 100/N_{sa}$, while the noise power is computed from (6) as P_n/σ_n^2. Clearly, the SNR is reduced as the overlap increases which is due to the correlation effect mentioned earlier. The trend of the curve is piecewise linear in dB, the slope shows a first discontinuity at $50\,\%$ overlap, which is the point at which the number of channels per overlapping element increases by one; here one elements starts contributing to three channels instead of two.

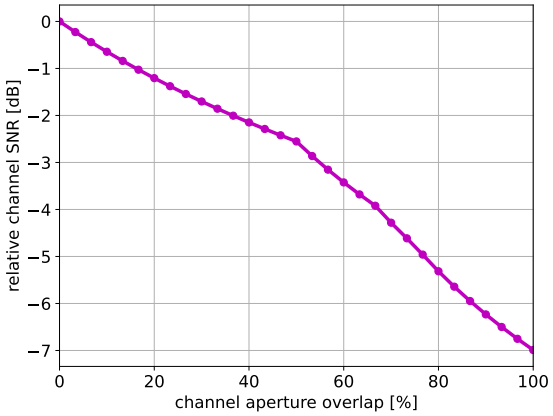

Figure 3: Relative channel signal-to-noise ratio versus percentage aperture overlap for an $N_{ch} = 5$ channel instrument with $N_{sa} = 30$ sub-array antenna elements.

3.2 Uniform PRF and Antenna Length

As the overlap between the channels increases the azimuth phase center separation is reduced. As a consequence the uniform PRF increases with increasing overlap between the channels, cf. (7). The uniform PRF normalized to that of an antenna without an overlap is given by:

$$\frac{f_{prf}^{uni}}{f_{prf}^{uni}\big|_{N_{ov}=0}} = \frac{1}{1 - \frac{N_{ov}}{N_{sa}}} \tag{9}$$

The above expression is plotted on the left ordinate of Fig. 4 versus the percentage overlap. It shows that introducing an overlap allows increasing the PRF. The right ordinate of Fig. 4 shows that the total antenna length is reduced in proportion to the overlap. As indicated before the antenna channel beamwidth, $\Phi \propto \lambda/L_{Rx}N_{sa}$, is assumed constant, which is the reason why the total antenna length is reduced when increasing the overlap.
Introducing an overlap thus allows shortening the antenna and increasing the uniform PRF. The former is an advantage for spaceborne systems, while the latter results in an increased data rate (for the same swath width) and may introduces timing constraints which require adding bursts to image the required swath at the cost of a worsened azimuth resolution. In general it can be said, that the uniform PRF of an instrument without overlap is matched to the received Doppler bandwidth as determined by the sub-array length. Introducing an overlap to increase the PRF, and by this the azimuth sampling, will allow better suppression of the azimuth ambiguities.

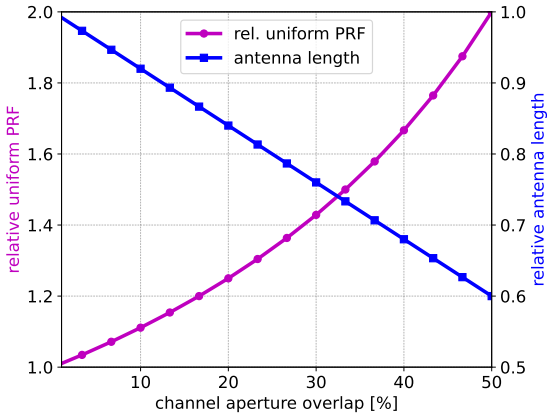

Figure 4: Relative uniform PRF value (left ordinate) and total antenna length (right ordinate) versus percentage aperture overlap for an $N_{ch} = 5$ channel instrument with $N_{sa} = 30$ sub-array antenna elements.

3.3 SNR Scaling Comparison

In the following we compare the SNR scaling of two 5-channel SAR systems: System A utilizes overlapping channels and operates at the uniform PRF, while system B has contiguous (non-overlapping) antenna elements, a longer antenna, but operates at the same PRF as system A, resulting in a periodic nonuniform sampling.

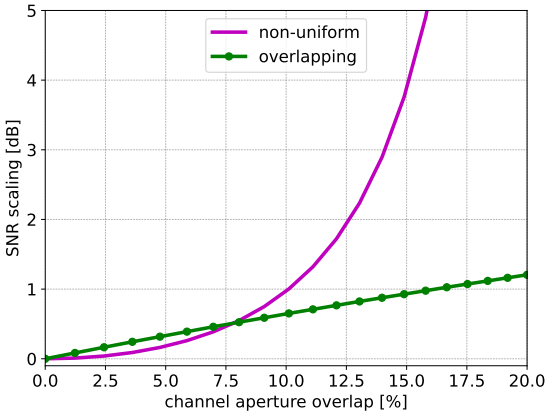

Figure 5: SNR scaling of two SAR systems operating at the same PRF.

Fig. 5 shows the SNR scaling (degradation) of both system versus the percentage overlap of system A. Here the nonuniformity of system B is converted to an equivalent percentage overlap according to $100(\gamma - 1)/\gamma$. It is seen that the SNR degradation due to the nonuniform azimuth sampling is, in general, higher than the degradation due to the overlapping channels (noise correlation).

4 Conclusion

Introducing an overlap between the azimuth channels of a synthetic aperture radar antenna results in an increased azimuth sampling rate and a higher value of the uniform

PRF which is favorable for suppressing the azimuth ambiguities. As shown here, this comes at the cost of a degraded signal-to-noise ratio, because the noise between the channels is no longer uncorrelated. It is suggested that it is not sufficient to look at individual SAR performance parameters but instead a comprehensive analysis of the complete trade-space is necessary to arrive at a conclusion concerning the advantages of this method.

References

[1] N. Gebert, "Multi-channel azimuth processing for high-resolution wide-swath SAR imaging," Ph.D. dissertation, German Aerospace Center (DLR), Aug. 2009.

[2] G. Krieger, N. Gebert, and A. Moreira, "Unambiguous SAR signal reconstruction from non-uniform displaced phase centre sampling," *IEEE Geoscience and Remote Sensing Letters*, vol. 1, no. 4, pp. 260–264, Oct. 2004.

[3] M. Younis, "NESZ-formulation for planar multi-channel SAR," German Aerospace Center, Microwaves and Radar Institute, Technical Note HR-RK-TN MY101, issue 2.3, Apr. 2019.

[4] ——, "Digital beam-forming for high resolution wide swath real and synthetic aperture radar," Ph.D. dissertation, Institut für Höchstfrequenztechnik und Elektronik, Universität Karlsruhe, July 2004.

[5] M. Younis, P. López-Dekker, F. Bordoni, P. Laskowski, and G. Krieger, "Exploring the trade-space of MIMO SAR," in *Proc. Int. Geoscience and Remote Sensing Symposium IGARSS'13*, Melbourne, Australia, July 2013.

[6] M. Younis and T. Bollian, "Circular orbit SAR geometry," German Aerospace Center, Microwaves and Radar Institute, Technical Note TN-RK-ST-TN7562, issue 1.6, Mar. 2022.

[7] J. Brown, "Multi-channel sampling of low-pass signals," *IEEE Transactions on Circuits and Systems*, vol. 28, no. 2, pp. 101–106, Feb. 1981.

[8] M. Younis, F. Bordoni, N. Gebert, and G. Krieger, "Smart multi-aperture radar techniques for space-borne remote sensing," in *Proc. Int. Geoscience and Remote Sensing Symposium IGARSS'08*, Boston, MA, USA., July 2008.

[9] G. Krieger, N. Gebert, and A. Moreira, "Multidimensional waveform encoding for synthetic aperture radar remote sensing," in *Proceedings of the IET International Conference on Radar Systems (RADAR)*, Edinburgh, UK, Oct. 2007.

[10] N. Gebert, G. Krieger, and A. Moreira, "Digital beamforming on receive: Techniques and optimization strategies for high-resolution wide-swath SAR imaging," *IEEE Transactions on Aerospace and Electronic Systems*, vol. 45, pp. 564–592, 2009.

[11] A. Papoulis, "Generalized sampling expansion," *IEEE Transactions on Circuits and Systems*, vol. 24, no. 11, pp. 652–654, Nov. 1977.

[12] D. Seidner and M. Feder, "Noise amplification of periodic nonuniform sampling," *IEEE Transactions on Signal Processing*, vol. 48, no. 1, pp. 275–277, Jan. 2000.

[13] ——, "Vector sampling expansion," *IEEE Transactions on Signal Processing*, vol. 48, no. 5, pp. 1401–1416, May 2000.